Geophys. J. Int. (1993) **114**, 304–310

Variations in upper mantle structure under northern Australia

S. C. Dey, B. L. N. Kennett, J. R. Bowman and A. Goody
Research School of Earth Sciences, Australian National University, Canberra, ACT 0200, Australia

Accepted 1993 January 5. Received 1992 December 29; in original form 1992 October 21

SUMMARY

Temporary array deployments of short-period seismometers in northern Australia have been used to build up composite record sections for waves interacting with the upper mantle. Stable measures of the seismic wavefield are provided by stacking the complex envelopes of all the seismic waveforms falling in a 10 km distance interval away from the source.

Two groups of sources (a) along the Flores Arc, Indonesia with propagation under northwestern Australia, and (b) in New Guinea with paths to the NNE of the array, have been used to construct composite record sections for both *P* and *SV* waves over the distance range 1300–2800 km. The timing and amplitude distributions for *P* waves from the two regions show noticeable differences. Detailed modelling of the record sections yields velocity models with significant variation in velocity for the two sets of propagation paths for which the midpoints are separated by about 1000 km.

The short-period *SV*-wave sections indicate efficient propagation of high-frequency *S* waves in a lithosphere extending down to 210 km. Arrivals from the deeper mantle cannot be correlated with confidence because of a loss in high-frequency content revealed by broad-band observations. This requires a significant attenuation zone for *S* beneath 210 km.

Key words: Australia, lateral heterogeneity, *P* waves, *SV* waves, upper mantle structure.

INTRODUCTION

The upper part of the mantle is cut by cold subducting slabs with high seismic velocities; where hot material is upwelling beneath rifts or in hot spots the seismic velocities are reduced. Even away from these prominent features there is significant heterogeneity in structure. Global tomography studies (e.g. Woodhouse & Dziewonski 1984) have revealed significant variations in the seismic wavespeeds in the upper mantle or scales of 1000 km or more, but currently still have rather limited depth resolution.

Studies of refracted waves provide the most direct approach to mapping horizontal variations in upper mantle velocities but require a favourable geometry of sources and receivers. By combining direct mantle observations of *SH* waves with those of the surface multiple *SS* at larger distances, Grand & Helmberger (1984) have been able to show significant differences in radial structure beneath the shield and tectonic regions of North America. A strong contrast across a tectonic boundary was also found in Europe (Rial, Grand & Helmberger 1984). Most of such upper mantle studies have been acquired using long-period waveforms because these are more stable and are less influenced by small-scale heterogeneity. However, the long period waves have wavelengths of the order of 100 km, at a depth of 400 km in the mantle, and this is not sufficient to determine the details of the transitions in the mantle. By contrast, short-period observations have greater potential resolving power but are also more susceptible to the effects of heterogeneity in structure. The influence of such heterogeneity can be reduced by building composite record sections for many events across a broad aperture recording array (Bowman & Kennett 1990).

The major earthquake belt running through Indonesia, New Guinea and its offshore islands lies at the appropriate distance range to investigate upper mantle structure using arrays of recording stations in northern Australia. The activity in this belt is such that a three-month deployment of temporary stations normally allows the preparation of a composite record section using events with magnitudes between 4 and 5.

This paper presents the results of two such field deployments to contrast the propagation characteristics of paths from the Flores Arc, Indonesia (previously studied by

Bowman & Kennett 1990) with paths from New Guinea. The turning points for waves bottoming in the upper mantle from these different groups of events are separated by about 1000 km. The resulting composite record sections show clear differences in timing and amplitude distribution for *P*-wave arrivals, which indicate differences in structure within the upper mantle.

TEMPORARY ARRAY EXPERIMENTS

Two separate deployments of temporary arrays of short-period instruments (LTC, NWB) were installed in the Northern Territory of Australia to record events in the Indonesia/New Guinea earthquake belt (Fig. 1). Each experiment had an aperture of around 400 km and lasted about three months. The array configurations follow the main highways to provide reasonable access to sites; each consisted of analogue recorders with 30–40 km spacing with a denser digital recorder array with 5–10 km spacing. The digital arrays were linked to the permanent Warramunga array (WRA—a 25 km aperture array of 20 short-period instruments) which lies about 50 km to the south of the intersection of the two arms of the recorder pattern in Fig. 1. The permanent array provides a useful supplement to the more widely spread stations in the temporary deployments.

For the LTC experiment from September to December 1985 the data comes primarily from the analogue recorders (the digital recorders did not perform well in the high temperatures of the tropical summer). For the NWB experiment from July to September 1986 much of the data used comes from the digital array and has been supplemented with analogue recordings to give a larger aperture.

The earthquakes for which data were extracted are displayed in Fig. 1. The events marked with a triangle were used by Bowman & Kennett (1990) to generate the *P*-velocity model NWB-1 for paths from the Flores Arc to northern Australia. The diamonds indicate additional events used in the construction of record sections for propagation paths to the LTC and NWB arrays.

The events chosen have NEIC body wave magnitudes between 4 and 5 with the object of trying to secure simple waveforms. However, a disadvantage of working with events of this size is that locations from global observations are of limited reliability. The uncertainties introduced by possible mislocation can be reduced by combining data from many events. The earthquakes have been chosen to lie above 40 km depth so that the propagation paths would have the smallest possible interaction with the subduction-zone structures.

In the subsequent displays we present composite record sections for two major classes of events based on the work of Dey (1989). The first consists of events along the front of the Flores Arc from 110°–132°E, 6°–12°S, and the second comprises events in New Guinea from 134°–153°E, 0°–9°S. Both these groups of events cover a moderate span in azimuths. A third group with a smaller azimuthal dispersal lies through the Banda Arc towards the Philippines but this is not discussed here, because of the likely contamination of the propagation characteristics through the upper mantle by the complex pattern of subduction zones surrounding the Banda Sea.

The midpoints for propagation from the selected events lie beneath the Australian continent or continental shelf. For the Flores events the turning points in the mantle lie beneath the Kimberley ranges in northwestern Australia. The turning points for the events in New Guinea lie mostly beneath the Gulf of Carpentaria. There is a horizontal

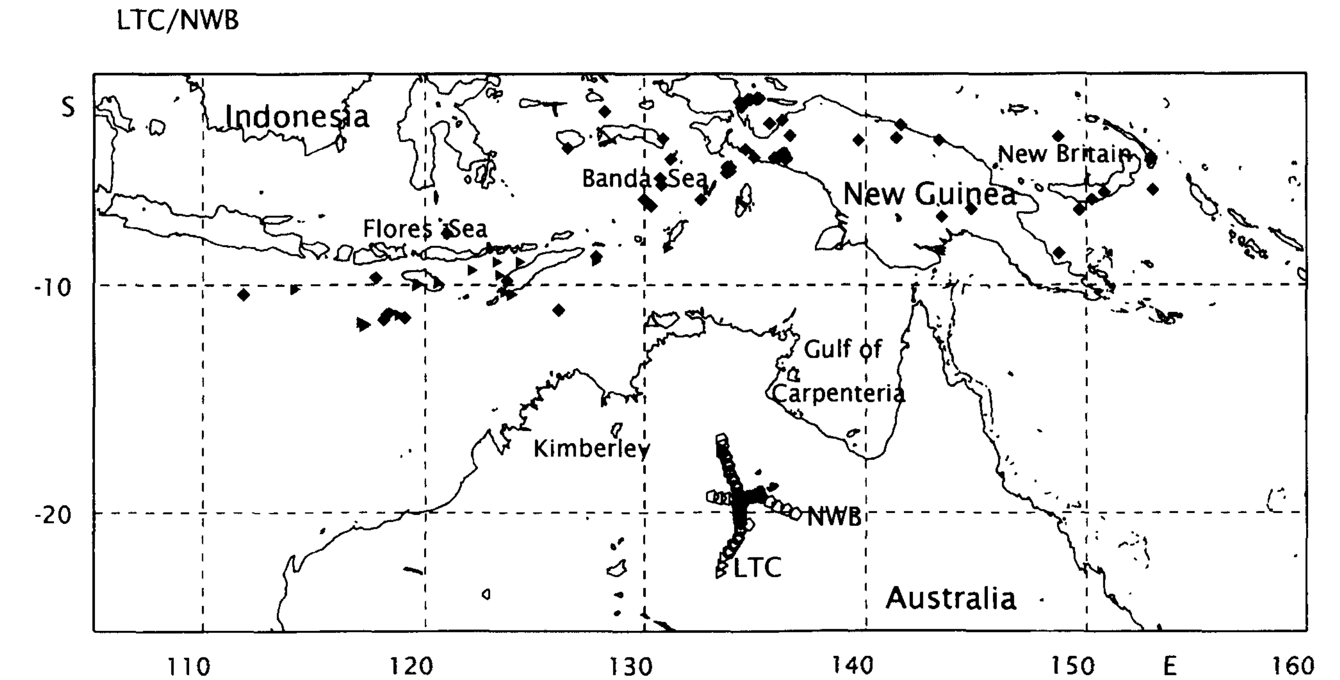

Figure 1. Earthquake distribution in the Indonesia–New Guinea region during the deployment of the portable arrays used in this study. The solid triangles denote the events used by Bowman & Kennett (1990) and the solid diamonds the events added for this study. The open triangles indicate the recorder locations in the LTC array and the pentagons the recorder locations for the NWB array.

separation between the two clusters of turning points of the order of 1000 km.

In order to gain the maximum coverage of the upper mantle we need to combine data from many events, and to do this we need to bring each event to a common depth. We have chosen to correct all events to surface focus based on an estimate of the mean slowness across the array of stations. This procedure is more successful for *P* waves than for the later *S* waves which suggests that there are residual errors in the depth and origin times for the events. Once each event has been corrected to surface focus, we have used stacking of all the arrivals in a narrow distance range to enhance the features of the composite record sections, particularly the later phases associated with mantle transitions. A very stable measure of the seismic wavefield is provided by a stack of the complex envelopes of those waveforms lying within 10 km distance bins (Bowman & Kennett 1990). This procedure reduces the influence of variations in source waveform and also counteracts the effects of small-scale heterogeneity. The stacking procedure has the consequence of lowering the apparent frequency of the data and imposing a slight delay on the location of amplitude maxima compared with unstacked data. The stacking procedure reduces the clutter in the record sections and allows a clear picture of the arrivals to been seen (Fig. 2).

Whilst the main emphasis here is on the radial structure in the upper mantle, we note that Kennett & Bowman (1990) have used the variation in amplitude distribution for individual events across arrays of different aperture and spacing to infer the presence of pervasive *P*-wave heterogeneity, of the order of 1 per cent with horizontal scale lengths of 200–300 km, superimposed on the main radial variation in velocity.

P-WAVE RECORD SECTIONS

Composite record sections for *P*-wave arrivals from the events along the Flores Arc, Indonesia and in New Guinea are compared in Fig. 2. Each trace is composed of a stack of the complex envelopes of all traces falling in a 10 km bin and is separately normalized to the maximum amplitude on the trace. Before stacking, all traces were filtered with a 0.5–3.5 Hz band pass. The application of depth corrections for each event prior to stacking has the effect of enhancing the arrivals on the later branches e.g. those associated with the 400 km discontinuity. Also, the depth corrections tend to suppress the influence of the surface-reflected phases *pP* and

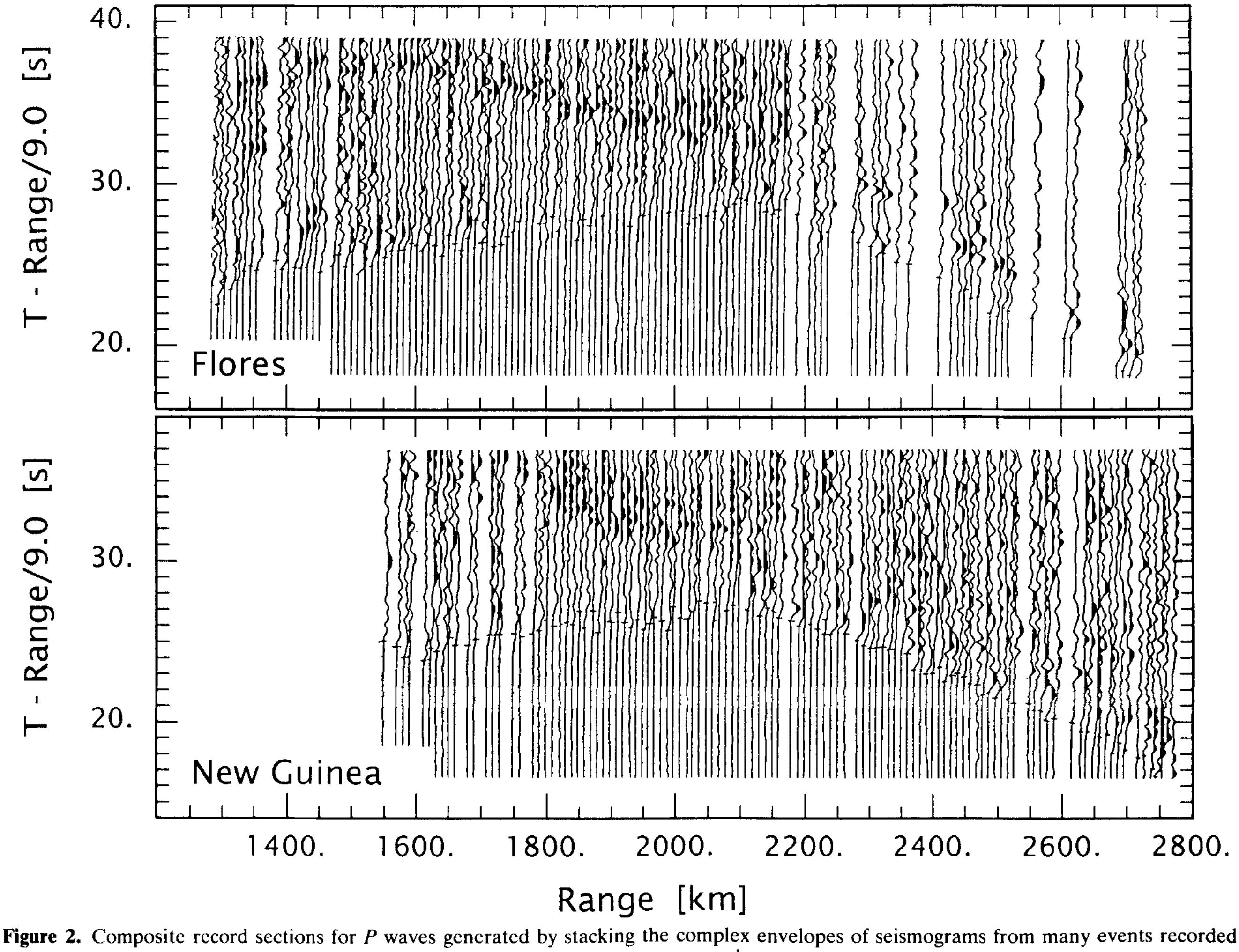

Figure 2. Composite record sections for *P* waves generated by stacking the complex envelopes of seismograms from many events recorded at the arrays of portable stations in northern Australia with reduction velocity 9 km s^{-1}, (a) events in the Flores Arc, Indonesia, (b) events in New Guinea.

sP which can be tracked across the records of a number of the individual events.

The data set for the Flores Arc presented in Fig. 2 is augmented from that used by Bowman & Kennett (1990) by the inclusion of some extra events. Much of the data used for the New Guinea section came from the LTC experiment because there were relatively few suitable events along the northern margin of New Guinea during the NWB recording period.

In Fig. 3, we present synthetic seismograms calculated for the *njp* reference model (Fig. 6) using the WKBJ technique (Chapman 1978) in order to provide a key to the main sets of arrivals in the composite sections in Fig. 2. We indicate the branches associated with each of the mantle discontinuities by a combination of the depth and suffix (*R* for the waves reflected back from the transition, *r* for waves refracted below the discontinuity). The reference model is chosen to give a general match to the character of both of the record sections, but is not intended to be a specific interpretation of either section.

Comparison of the *P*-record sections (Fig. 2) with the synthetics for the reference model (Fig. 3) shows significant differences in the timing and amplitude distribution between the sections for the sources in the Flores and New Guinea regions. A striking feature of both observed sections is the prominence of arrivals associated with the 410 km transition, but there is notable difference in the amplitude patterns in the two cases, and also the timing relative to the first arrivals. For the sources in the Flores Arc, with propagation through the zone to the northwest of the arrays, the refracted branch from below the 410 discontinuity (410r) is prominent out to 2000 km. For the sources in New Guinea to the NNE of the arrays, the retrograde reflected branch is larger in this distance interval; the refraction is more prominent beyond 2100 km as a first arrival. The larger reflected arrivals suggest that the contrast at the 410 km discontinuity may be generally larger for paths from New Guinea. The balance of the amplitude of different phase branches can be changed by the nature of the source mechanism but the two branches 410r, 410R have similar take-off angles. The consistency of amplitude patterns over several hundred kilometres helps with the association of the character of the record sections with structural features. However, it should be noted that Bowman & Kennett (1990) present records from two events in the Flores Arc with exceptionally clear arrivals from the 410 km transition but the majority of events have no such dramatic features.

At larger distances the differences in the sections arise in part from the event distribution during the recording periods. For the Flores Arc, most of the records beyond 2200 km come from just two events with prominent arrivals that can be associated with the '660 km' discontinuity. The branches for the reflected and refracted arrivals are rather close together in this range but the timing of the branches favour a discontinuity shallower than 660 km. For the New Guinea region, events in the New Britain subduction zone provide a much denser coverage at greater distances and there is more indication of the reflected branch (660R) than the corresponding refraction beneath the 660 km transition. The emergence of the 660r branch as a first arrival occurs just outside the distance range displayed in Fig. 2.

At short ranges there is much better data coverage from the sources in the Flores Arc and in consequence better evidence for the presence of a 210 km discontinuity to explain the separation between the onsets and the prominent energy 2 s or more later over the interval 1500–1700 km.

Since we recognize that the locations used in preparing the composite record sections may well have significant errors, we need to know how these may affect the character of the composite sections. To simulate the effects of the errors we have prepared sections with the location of the sources randomly perturbed by up to 0.3° from the original location. The character of the composite sections is preserved but there can be bulk time offsets of about a second. The modification of the locations is not sufficient to disturb the prominent features of the section which are controlled by the triplications in the traveltime curve.

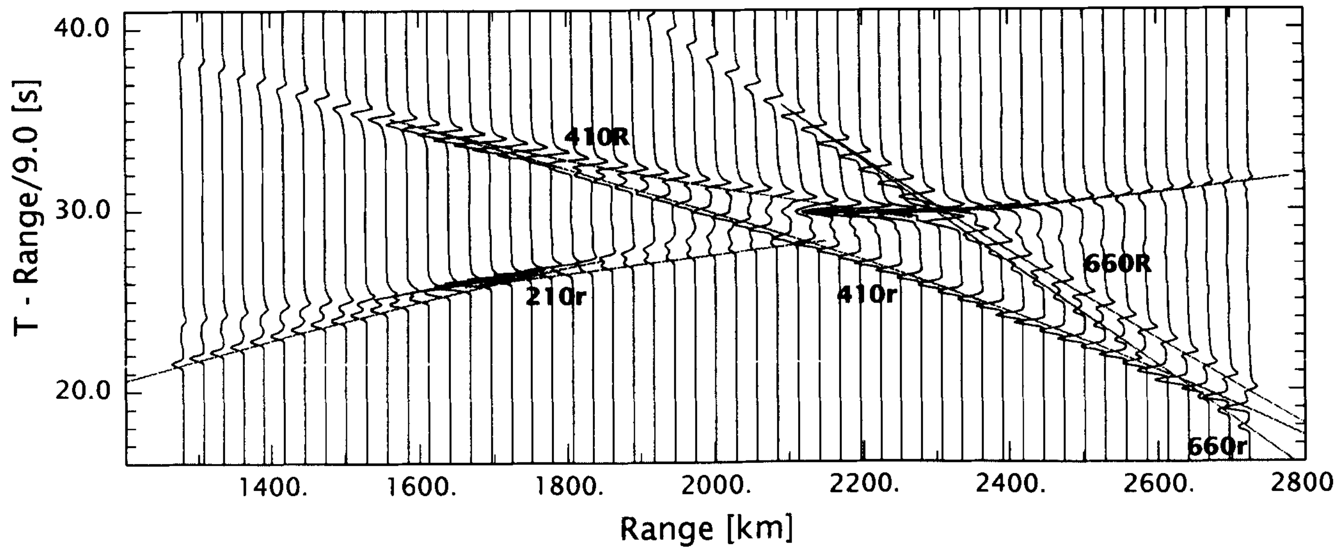

Figure 3. Theoretical seismogram section for *P* waves for the reference model *njp* calculated using WKBJ technique for a surface source. The traveltime branches are denoted by the discontinuity with which they are associated (*r*—refraction below, *R*—retrograde reflection).

Although we have presented theoretical seismograms for a perfectly elastic medium for comparison with the record sections of Fig. 3, the interpretations leading to the velocity models (*fls*—Flores section, *ngr*—New Guinea section) shown in Fig. 6 were based in part on reflectivity calculations including attenuation. There can be a significant trade-off between the details of velocity structure and attenuation (see e.g. Kennett 1975), but broad-band observations at the Warramunga array (Goody 1991) do not suggest the need for any significant zones of increased attenuation for *P* waves.

SV-WAVE RECORD SECTIONS

Using a similar set of procedures to those used to construct the composite *P*-wave sections (Fig. 2) we have attempted to generate composite record sections for mantle *S* arrivals from both the Flores and New Guinea source regions. The complex envelope stacks of the *S*-wave arrivals from the vertical component seismometers in the temporary arrays are displayed in Fig. 4. Three-component data was only available from the permanent Warramunga array and was not sufficient to create record-sections from the horizontal components.

Although the *SV*-wave sections of Fig. 4 have nothing like the clarity of the *P*-wave sections, they do show some consistent features. We note that the *S* waves from the sources in New Guinea appear to have slightly lower frequency than those from the sources in the Flores Arc. There is moderately coherent high-frequency propagation for *S* out to about 2200 km, thereafter it is difficult to correlate arrivals. There are hints of later branches, but on these short-period records it is difficult to have confidence in any particular choices. Part of the problem arises because trace alignment before stacking has not been as effective as for *P*, the corrections are larger and therefore errors in location parameters have greater effect. However, the main problem arises from the lower-frequency content of the waves returned from the deeper-mantle discontinuities.

A broad-band seismometer (Guralp CMG-3) has been operated at the Warramunga array since 1988 and there is now sufficient data to build up three-component record sections (Goody 1991). High-frequency *S* waves are recorded as the onset of the *S* waveform from both *SV* and *SH* waves out to 2200 km. At larger distances the onset of *S* has much lower-frequency content (0.25–0.3 Hz) and such intermediate period arrivals characterize the *S* waves returned from the 410 and 660 km discontinuities.

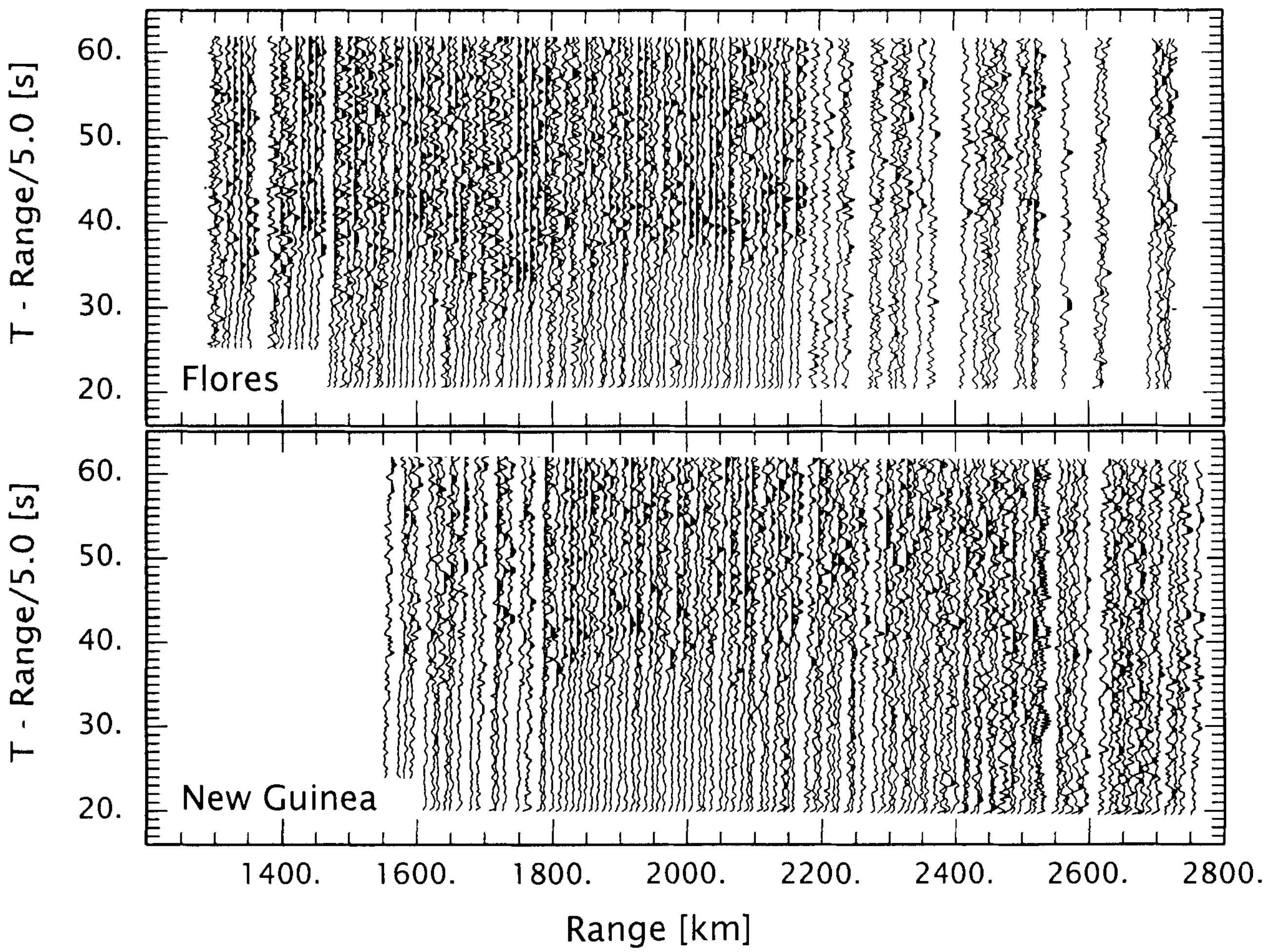

Figure 4. Composite record sections for *S* waves generated by stacking the complex envelopes of seismograms from many events recorded at the arrays of portable stations in northern Australia with reduction velocity 5 km s^{-1}, (a) events in the Flores Arc, Indonesia, (b) events in New Guinea.

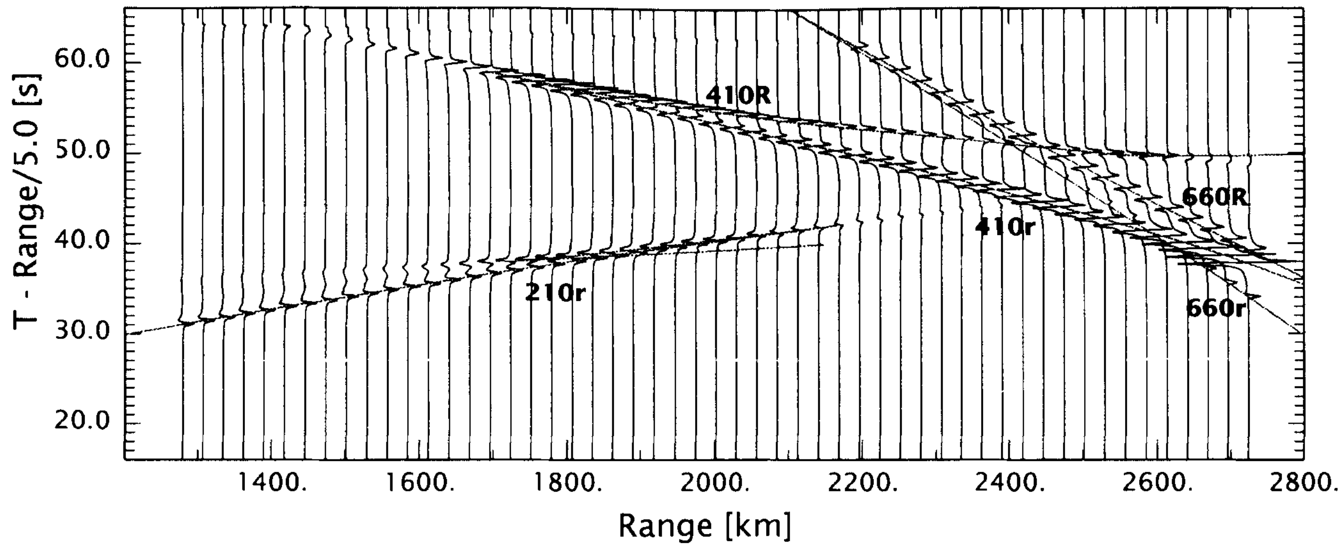

Figure 5. Theoretical seismogram section for *S* waves for the reference model *njp* calculated using WKBJ technique for a surface source. The traveltime branches are denoted by the discontinuity with which they are associated (*r*—refraction below, *R*—retrograde reflection).

WKBJ seismograms for the reference model *njp* (based on the broad-band results) are displayed in Fig. 5 to provide a guide to the expected locations of arrivals from deeper discontinuities. No attenuation has been included in the synthetic seismogram calculations in Fig. 5. The dramatic loss of high frequencies for the 410 and 660 km arrivals requires the presence of significant attenuation in the zone below 210 km. The times for the 210 km arrivals give a good general match to the observations, occasional high-frequency arrivals beyond 2200 km are consistent with surface multiples trapped in a high *Q* lithosphere extending down to 210 km.

With the insight provided by the constraints from the broad-band data it is possible to find reasonable correlations of features in the *S*-wave sections with the theoretical times. For example, the 410r branch between 1800 and 2100 km for reduced times around 55 s may be evident in the data of Fig. 4 but it would have been difficult to sustain this correlation without additional information.

DISCUSSION

In the two previous sections we have displayed composite record sections for *P*- and *S*-wave propagation through the upper mantle from sources in the Flores Arc, Indonesia and New Guinea to arrays of stations in northern Australia.

The record sections indicate noticeable differences for the propagation characteristics from the two sets of sources both in the relative timing of phase branches and the amplitude distribution between branches. Detailed modelling of the *P*-wave sections using synthetic-seismogram matching of the times and amplitude characteristics, following the procedures discussed by Bowman & Kennett (1990), has led to the construction of two distinct models for the Flores and New Guinea profiles. The *P*-wave velocity models *fls*—Flores, *ngr*—New Guinea are displayed in Fig. 6 together with the reference model *njp* used for the preparation of the theoretical seismogram sections in Figs 3 and 5.

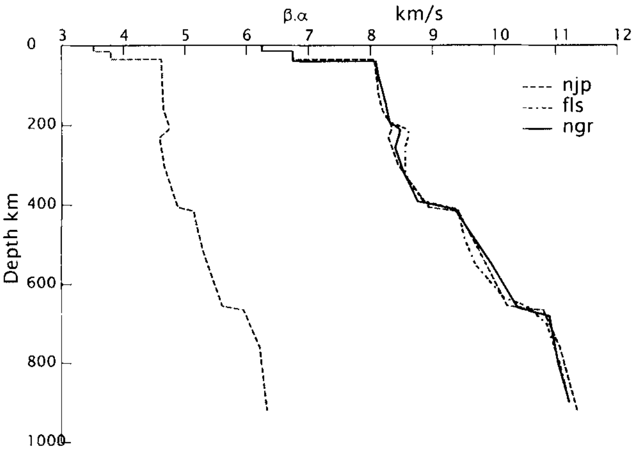

Figure 6. Comparison of velocity models for the northern Australian region. The *P*-wave models *fls*, *ngr* deduced by modelling the features of the composite record sections in Fig. 3 are compared with the reference model *njp* used to prepare the theoretical seismogram sections in Figs 3 and 5. The features of the *S*-wave velocity distribution below 210 km are derived from modelling of broad-band observations.

The *P*-wave models, derived from the detailed analysis of the record sections, sustain the differences in structure suggested by the earlier work of Bowman & Kennett (1990) for sources in the Flores Arc, and the slowness and traveltime studies of Simpson, Mereu & King (1974) for sources in New Guinea observed at the Warramunga array.

The *P* models are well controlled to a depth of about 550 km, since the available aperture is not sufficient to give a good resolution of the structure at the 660 km discontinuity. The differences in upper mantle structure below 210 km summarized by the differences between the *fls* and *ngr* models occur over a horizontal distance of about 1000 km (the separation between the clusters of midpoints for the two profiles). The differences in the models imply significant medium-scale variability within the upper mantle.

The *fls* model is very close to the NWB-1 model of Bowman & Kennett (1990) but the shallow structure which is not constrained by the available data has been modified slightly. The inclusion of an additional event at larger range has also led to a slightly deeper '660' km discontinuity, though still somewhat shallower than for *ngr*. A prominent 210 km discontinuity is needed for paths through north-western Australia (Hales, Muirhead & Rynn 1980; Leven 1985) but only a slight transition is required to match the character of the New Guinea profile. The large differences in amplitude between the 210 r branch and the arrivals from the 410 km discontinuity require a zone of reduced velocity gradients below 210 km.

The *ngr* model is generally similar to SMAK-1 (Simpson *et al.* 1974) but has sharper discontinuities, which have been modelled as gradient zones over a 10 km interval. A lower velocity than for *fls* is required at 210 km to match the apparent velocity of the first arrivals between 1800 and 2200 km range. The gradient above the 410 km discontinuity is quite low and a large contrast at the discontinuity than for *fls* is included to match the enhanced amplitudes on the 410 R branch in Fig. 3. Below the 410 km discontinuity the velocity is slightly higher at first in the *fls* but the *ngr* model is faster at depth.

The differences in the size of the feature in the P-wave-speed distributions for *fls* and *ngr* near 210 km depth may well be associated with anisotropy at the base of the lithosphere as suggested by Leven, Jackson & Ringwood (1981). The presence of such anisotropy is supported by consistent observations of about 1 s shear wave splitting between SV and SH arrivals observed on broad-band records for the 210R branch (Goody 1991). Such splitting is not observed consistently from deeper structure.

For S-wave propagation we have been able to enhance the interpretation of the short-period data by incorporating additional information from three-component broad-band recordings. The general character of the S sections is similar, although the arrivals from New Guinea tend to be of slightly lower frequency. There is efficient high-frequency propagation of SV in the lithosphere (down to 210 km) and the comparative absence of deeper mantle arrivals can be explained by a frequency shift to intermediate periods due to attenuation below 210 km. Unfortunately we do not have enough information at this stage to tell whether the S-wave structures at depth mirror those of the P-wave velocity distribution.

REFERENCES

Bowman, J. R. & Kennett, B. L. N., 1990. An investigation of the upper mantle beneath NW Australia using a hybrid seismograph array, *Geophys. J. Int.*, **101**, 411–424.

Chapman, C. H., 1978. A new method for computing synthetic seismograms. *Geophys. J. R. astr. Soc.*, **54**, 431–518.

Dey, S. C., 1989. Lateral variations in the upper mantle velocity structure under northern Australia, *PhD thesis,* Australia National University.

Goody, A., 1991, Broad-band studies of the upper mantle beneath northern Australia, *Honours thesis,* Australian National University.

Grand, S. & Helmberger, D. V., 1984. Upper mantle shear structure of North America, *Geophys. J. R. astr. Soc.*, **76**, 399–438.

Hales, A. L., Muirhead, K. J. & Rynn, J. W., 1980. A compressional velocity distribution for the upper mantle, *Tectonophysics*, **63**, 309–348.

Kennett, B. L. N., 1975. The effects of attenuation on seismograms, *Bull. seism. Soc. Am.*, **65**, 1643–1651.

Kennett, B. L. N. & Bowman, J. R., 1990. The velocity structure and heterogeneity of the mantle, *Phys. Earth planet. Inter.*, **59**, 429–465.

Leven, J. H., 1985. The application of synthetic seismograms in the interpretation of the upper mantle P-wave velocity structure in northern Australia, *Phys. Earth. planet. Inter.*, **38**, 9–27.

Leven, J. H., Jackson, I. & Ringwood, A. E., 1981. Upper mantle seismic anisotropy and lithospheric decoupling, *Nature*, **289**, 234–239.

Rial, J. A., Grand, S. & Helmberger, D. V., 1984. A note on lateral variation in upper mantle shear-wave velocity across the Alpine front, *Geophys. J. R. astr. Soc.*, **77**, 639–654.

Simpson, D. W., Mereu, R. F. & King, D. W., 1974. An array study of P wave velocities in the upper mantle transition zone beneath northeastern Australia, *Bull. seism. Soc. Am.*, **64**, 1757–1788.

Woodhouse, J. H. & Dziewonski, A. M., 1984. Mapping the upper mantle, three dimensional modelling of Earth structure by inversion of seismic waveforms, *J. geophys. Res.*, **89**, 5953–5986.